DOI: 10.1002/anie.201204983

Gel–Air Electrodes

From Li–O_2 to Li–Air Batteries: Carbon Nanotubes/Ionic Liquid Gels with a Tricontinuous Passage of Electrons, Ions, and Oxygen**

*Tao Zhang and Haoshen Zhou**

Li–O_2 batteries are attracting intensive attention because their theoretical large energy density, based on the reversible reaction of $2\,Li + O_2 \rightleftharpoons Li_2O_2$, is 3505 Wh kg^{-1}, which is about eight times larger than those of the C/$LiMn_2O_4$ (or C/$LiCoO_2$, C/$LiFePO_4$) series of rechargeable lithium-ion batteries.[1] However, there are many critical drawbacks that limit the application of the now-established lithium–O_2 battery: 1) The conventional organic liquid electrolytes are volatile, and will be exhausted in an open system such as a Li–O_2 battery; 2) the decomposition of the organic electrolytes during discharge and charge processes makes the battery unstable and the electrolytes are consumed;[2] and 3) the liquid electrolyte readily permeates into the pores of air electrodes, which is necessary to provide the necessary lithium ions. However, once the pore in an air electrode is completely filled with liquid electrolyte, the diffusion of oxygen is blocked.[3] This results in the electrochemical reaction being based solely on the dissolved oxygen gas in the electrolyte (Figure 1 a), which results in large polarization, safety problems from corrosion of the anode, poor rate performance, and weak reversibility. Moreover, it also prevents extension to a lithium–air battery in ambient, humid air. This is the reason why most non-aqueous lithium–air batteries are investigated in pure O_2, and are thus called as Li–O_2 batteries.

To overcome the first and second drawbacks, the ionic liquid (IL) 1-ethyl-3-methylimidazolium bis(trifluoromethylsulfonyl) ([C_2C_1im][NTf_2]) is chosen as the electrolyte in Li–O_2 batteries to replace the conventional liquid electrolytes of commercial lithium-ion batteries. This ionic liquid is used because of its excellent nonvolatility, high hydrophobicity against water, high thermal stability, and broad electrochemical window.[4] We designed single-walled carbon nanotubes (SWNTs) and the corresponding [C_2C_1im][NTf_2] cross-linked network gel (CNG) for the oxygen electrode of a Li–O_2 battery to solve the third main drawback. Here, the SWNTs are regarded not only as the support for the discharge products, similar to other carbonaceous materials,[5] but also as being critical for the conductive passage of electrons because SWNTs have a well-defined atomic structure, high length to diameter ratio,[6] and high electroconductivity (10^2–10^3 S cm^{-1}).[7] Moreover, in comparison to the typically highly tangled SWNT bundles[8] that have a reduced effective surface area, the SWNTs in the CNG are untangled upon being ground into the imidazolium ion based [C_2C_1im][NTf_2] IL to form the gel. This untangling possibly occurs through specific interactions[9] between the cation in the [C_2C_1im]-[NTf_2] IL and the π-electronic surface of the nanotubes (see Figures S1 and S2 in the Supporting Information).

More importantly, the permeation of the IL from the IL electrolyte into the CNG could be excellently suppressed (Figure 1 b) because of the existing anchored IL in the CNG. Immersion of the CNG in the IL electrolyte for one week resulted in its weight increasing just from permeation of the Li salt, that is by 0.37 M in the CNG, which is almost consistent with the 0.5 M concentration in the IL electrolyte (for a detailed explanation, see Figure S3 in the Supporting Information). A schematic representation of the application of the SWNT/IL CNG as the air cathode of a Li–O_2 battery is illustrated in Figure 1 c,d, and can be characterized by three main aspects: 1) the SWNTs allow the efficient passage of electrons, 2) the ([C_2C_1im][NTf_2]) IL, which is anchored to the SWNTs through molecular ordering and hence interconnects neighboring SWNTs nanowires,[7,9] is responsible for the high conduction of lithium ions within the SWNT/IL CNG, and 3) the cross-linked SWNT/IL networks allow the passage of oxygen, not through oxygen dissolution, but through the indispensable oxygen diffusion channels arising from the numerous small chinks and pores within the SWNT/IL CNG. The conventional three-phase electrochemical interface could be expanded into 3-dimentional networks in whole SWNT/IL CNGs, which may allow the "three dimensional tricontinuous passage of electrons, ions, and oxygen", which would greatly widen the conventional electrochemistry of oxygen in Li–O_2 batteries.

A comparison of the discharge/charge behavior of SWNT/IL CNGs and a commonly used mixture of SWNTs and IL is shown in Figure 2 a. The cells were operated in 1 atm O_2 with a cut-off voltage from 2.0 to 4.0 V versus the Li/Li$^+$ couple. The discharge capacity of the SWNT/IL CNG reached 5930 mAh g^{-1}, which is over six times that of the SWNT/IL mixture (950 mAh g^{-1}), and explicitly gives electrochemical evidence that the ability of the SWNTs to accommodate discharge products was greatly increased after the SWNTs bundles were completely dispersed to allow the tricontinuous passage. In terms of discharge products, the powder X-ray diffraction (XRD) patterns of Li_2O_2 were clearly observed (see the inset of Figure 2 a). Moreover, the four strong peaks of Li_2O_2 all disappeared after charging to 4.0 V versus the Li/

---

[*] Dr. T. Zhang, Prof. H. Zhou
Energy Technology Research Institute, National Institute of
Advanced Industrial Science and Technology (AIST)
Umezono 1-1-1, Tsukuba, 305-8568 (Japan)
E-mail: hs.zhou@aist.go.jp

[**] This work was partially supported financially by the Funding Program for World-Leading Innovative R&D on Science and Technology (FIRST). We thank Sumika Chemical Analysis Service, Ltd. for TEM measurements.

Supporting information for this article is available on the WWW under http://dx.doi.org/10.1002/anie.201204983.

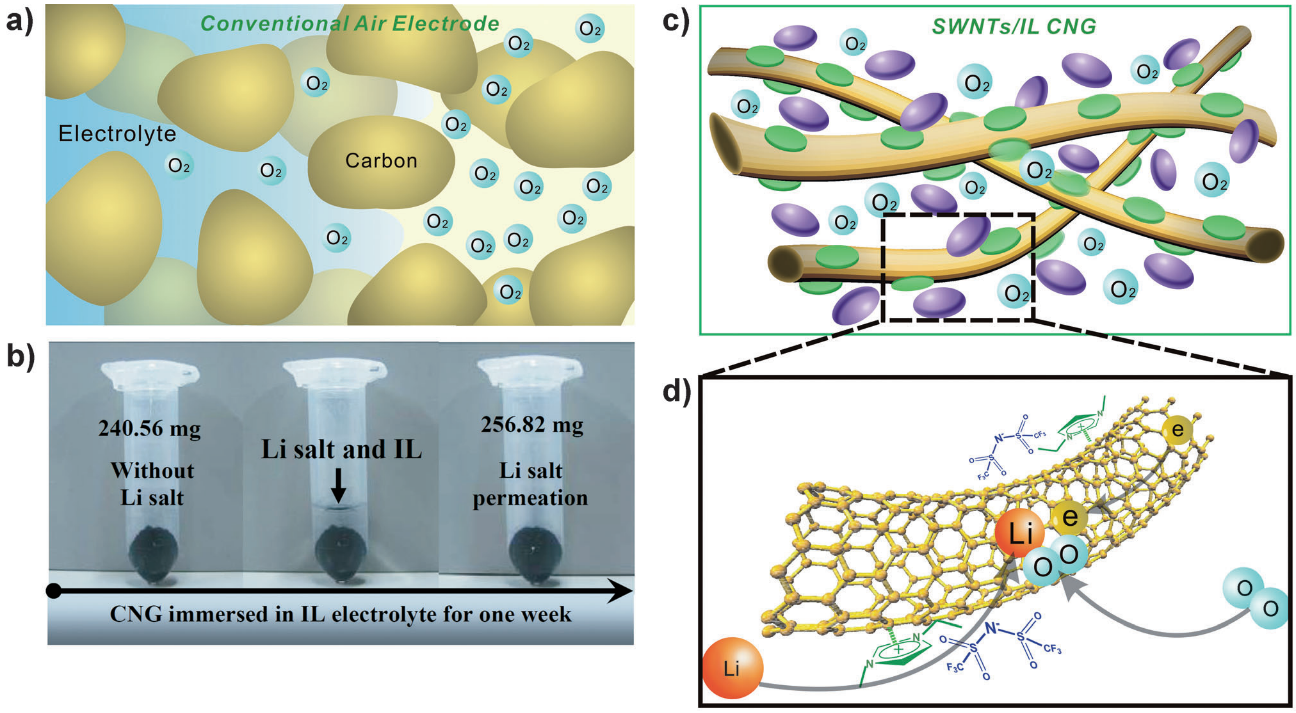

Figure 1. Schematic representations comparing the conventional air electrode with the SWNT/[C_2C_1im][NTf_2] CNG air electrode. a) Air electrode using a conventional carbonaceous material such as acetylene black. The three-phase interfacial reaction is confined by the dissolved oxygen. b) Weight variation of the SWNT/[C_2C_1im][NTf_2] CNG after immersion in an electrolyte of 0.5 M Li[NTf_2] salt and [C_2C_1im][NTf_2] for one week. c) SWNT/[C_2C_1im][NTf_2] CNG. SWNTs (gold) were untangled by a π–cation/π–electron interaction with the imidazolium cation of [C_2C_1im]$^+$ (green), thereby forming physical gels with cross-linked networks. The [NTf_2]$^-$ ions (purple) were anchored in the gel through electric neutrality. Oxygen fills the entire cross-linked network gel. d) Three dimensional tricontinuous passage of electrons, ions, and oxygen. Electrons conduct along the carbon nanotubes. Lithium ions transferred from the ionic liquid electrolyte outside into the cross-linked network gel become coordinated by the inside-anchored [NTf_2]$^-$ ion. Oxygen in the cross-linked network incorporates with the lithium ions and electrons along the SWNTs, thereby turning into the discharge products.

Li^+ couple. A reversible reaction of $Li + O_2 \rightleftharpoons Li_2O_2$ was observed, thus providing a possibility to introduce SWNT/IL CNGs into Li–O_2 batteries.

We noticed that the SWNT/IL cross-linker showed an alleviating hysteresis between the discharge and charge voltages (Figure 2a), since the deviation of the mid-potential of 1.07 V at a current density of 200 mAg^{-1} is apparently lower than the common value of about 1.50 V derived from porous carbon carriers.[10] Furthermore, it should be noted that no catalysts, such as perovskite oxide,[5b] Pt/Au,[10] and α-MnO_2,[11] facilitate the electrochemistry of the oxygen in the SWNT/IL CNGs. Therefore, the improvement in the electrical energy efficiency of the discharge/charge process can be credited in a large part to contributions made by the configurational features of the SWNT/IL CNGs.

A further hint that the SWNT/IL CNGs may bring an improvement at the reactive interface of the Li–O_2 cell came from the very low interfacial resistance of 355 mΩcm^2 between the IL electrolyte and the SWNT/IL CNG cathode (see Figure S5 in the Supporting Information), which prompted us to investigate the rate performance of the Li–O_2 cell. Figure 2b shows that the Li–O_2 cells based on the SWNT/IL CNG maintained a continuous useful discharge platform with increasing current densities. A discharge capacity of 2020 mAhg^{-1} was still obtained at a high current density of 2000 mAg^{-1}. So far the majority of research on Li–O_2 batteries[11,12] limited the current densities to lower than 200 mAg_{carbon}^{-1}. Even if the rate performance was investigated, it was confined only to the discharge process.[13] However, the SWNT/IL CNG herein maintained a striking discharge/charge columbic efficiency of 64% at 2000 mAg^{-1}, which is thus far the highest rate capability with partial reversibility. This finding suggests that the neoteric structure with a "three-dimensional tricontinuous passage of electrons, ions, and oxygen" is beneficial not only for the reduction of oxygen, but also for the evolution of oxygen.

Discharge platforms similar to acetylene black[11,12] of approximately 2.70–2.50 V were observed for the SWNT/IL CNG when discharged within a low current range of 0 to 200 mAg^{-1}. In general, the charge transfer is the rate-controlling process at low current densities. However, when the current density increases, the mass transfer, including of lithium ions and oxygen, becomes the main controlling process. As a complex solid–liquid–gas heterogeneous reaction, the reaction velocities of $Li + O_2 \rightleftharpoons Li_2O_2$ refers saliently to the unit interfacial area. The conventional support, similar to acetylene black, builds the interfacial area and depends, inevitably, on the permeation of the electrolytes into the support to provide lithium ions. The available oxygen is also confined to the dissolved oxygen molecules near to the interfacial area. In the case of the SWNT/IL CNG, the [C_2C_1im][NTf_2] anchored to the nanotube surface through

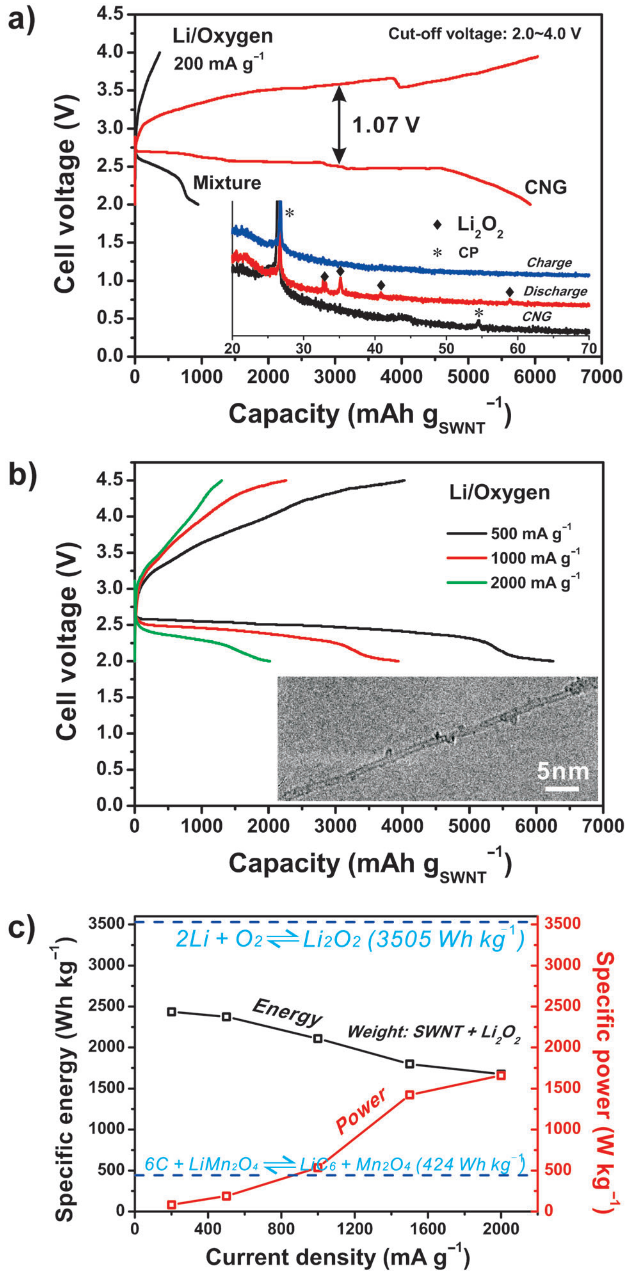

Figure 2. Discharge/charge performance and rate capability of the $Li–O_2$ cell. a) The discharge/charge curves of the $Li–O_2$ cell with the SWNT/[C_2C_1im][NTf_2] CNG and a mixture (before gelation) at 200 mAg_{SWNT}^{-1} in 1 atm O_2. The capacity was normalized by the weight of the SWNTs. The inset shows the corresponding XRD patterns of the SWNT/IL CNG loaded onto the carbon paper (CP) current collector before and after discharge/charge. b) The rate capability of the $Li–O_2$ cells with the SWNT/IL CNG at a gradual increase in the current densities from 500 to 2000 mAg_{SWNT}^{-1} in 1 atm O_2. The inset shows the SWNTs after discharging. Large particles of the discharge products separate away from the surface of the SWNTs through the ultrasonic treatment used for sample preparation (see Figure S4 in the Supporting Information). c) The corresponding specific energy and specific power of the $Li–O_2$ cells, which were calculated based on the total weight of the SWNTs and the resultant Li_2O_2.

a π-cation/π-electron interaction can be regarded as a special elongation of the same IL solvent in the electrolyte. The infiltration of the electrolyte into the CNG is suppressed, because of the occupancy of the anchored [C_2C_1im][NTf_2], but the transfer of lithium ions is still maintained smoothly under an applied potential. Synchronously, the CNG is a solid-state gel and provides expanded transfer space for the external oxygen, which diffuses along the surfaces of the SWNTs and IL gel to incorporate with lithium ions and electrons. As a consequence, the interfacial area is expanded to the whole network of the SWNT/IL CNG, which is suitable for high current flows.

Combining the discharge performance and rate capability stated above, the specific energy and power of the $Li–O_2$ cell with the SWNT/IL CNG can be assessed by integration (Figure 2c). The calculations were normalized by the total weight of the SWNTs and the resultant Li_2O_2. A specific energy of 2440 Wh kg^{-1} was obtained at 200 mA g^{-1}, which is around 70% of the theoretical value. It should be noted that the theoretical value is based solely on the weight of the Li_2O_2, but the determined value of 2440 Wh kg^{-1} is based on the weight of the Li_2O_2 and the SWNT support. This value is about six times as high as the theoretical value of a lithium-ion battery based on $6C + LiMn_2O_4 \rightleftharpoons LiC_6 + Mn_2O_4$, which is about 425 Wh kg^{-1} based on the weight of the active materials for the electrodes. It is also important to note that, from a specific energy point of view, the advantage will be impaired at a practical level by the higher packing weight factor of the $Li–O_2$ battery.[14] As the discharge rate increases, the specific power rises significantly. At 2000 mA g^{-1}, the specific power reached 1660 W kg^{-1}, also based on the weight of the SWNTs and the resultant Li_2O_2, while a substantial specific energy of 1680 Wh kg^{-1} still remains. The data are reminiscent of the usable specific energy of gasoline for automotive applications (ca. 1700 Wh kg^{-1}),[15] and are also desirable for approaching the general requirements of specific power (1000–1500 W kg^{-1}) for electric vehicles.

Recognizing that the superior “tricontinuous passage of electrons, ions, and oxygen” is the key to improve the specific energy and power of the $Li–O_2$ battery with a SWNT/IL CNG cathode, we further investigated its effects on the passage of H_2O and CO_2 in ambient air (oxygen partial pressure: 0.21 atm; humidity: ca. 50). The initial motivation was the finding that a water drop slid away from the surface of the SWNT/IL CNG. Further investigation indicated that the SWNT/IL CNG exhibits excellent water stability (Figure 3a). After immersing the CNG in deionized water for one week, its weight didn’t increase, but decreased from 256.82 mg to 247.77 mg, which results from about half of the Li salt in the CNG dissolving into the water (for a detailed explanation, see Figure S3 in the Supporting Information). The Li–air cell gave a large discharge capacity of 10200 mAh g^{-1} in ambient air (Figure 3b), which is twice that of the lithium–air cell with a porous graphene support in air.[16] The corresponding XRD pattern revealed that Li_2O_2 and LiOH formed during the discharge process in air (see the inset of Figure 3b). It is speculated that the stability of the macro water originated from the hydrophobicity of the anchored IL, but some H_2O molecules in air can still permeate into the SWNT/IL CNG by

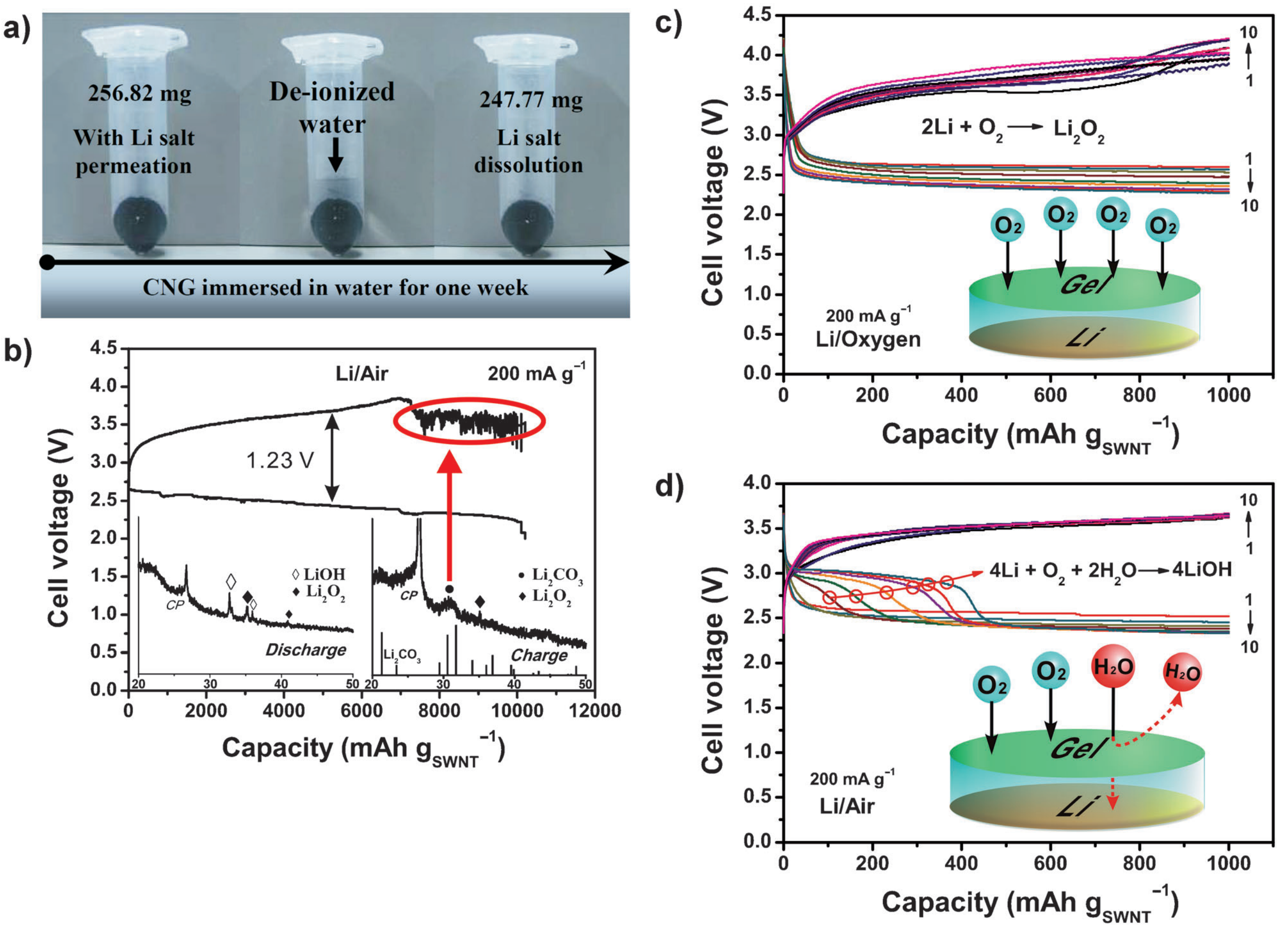

Figure 3. Analysis of the electrochemical behavior of the Li–air cell. a) Weight variation of the SWNT/[C_2C_1im][NTf_2] CNG after immersion in deionized water for one week. b) The discharge/charge curves of the Li–air cells with a SWNT/[C_2C_1im][NTf_2] CNG at 200 mA g_{SWNT}^{-1} in ambient air. The insets are the XRD patterns of the SWNT/IL CNG cathode after discharging and charging. c) The cycling performance of the Li–O_2 cell (1 atm O_2) at 200 mA g_{SWNT}^{-1} when the discharge and charge is limited to 1000 mAh g^{-1}. d) The cycling performance of the Li–air cell (ambient air) at 200 mA g_{SWNT}^{-1} when the discharge is limited to 1000 mAh g^{-1}. All of the capacities were normalized by the weight of the SWNTs. The insets in (c) and (d) illustrate the influence of the contamination from H_2O in the air on the Li–O_2 cells.

the passage of oxygen. Nevertheless, the stability of the macro water, determined by integrating the hydrophobic IL electrolytes, has laid a foundation towards operating Li–O_2 batteries in ambient air.

The charge curve in air was plagued by intensely scattered plots after 7260 mAh g^{-1} (Figure 3b). Thus, the XRD pattern of the air cathode in this region was investigated (see the inset of Figure 3b) to analyze the phenomenon. The peak corresponding to LiOH after discharge disappeared, but a peak corresponding to Li_2CO_3 was evident, which suggested contamination by CO_2 from the air. Thus, the unstable charge potential may be attributed partly to the insulation and irreversibility of Li_2CO_3. Moreover, the peak corresponding to Li_2O_2 after discharge became weaker, but remained. These results provide evidence that the following reactions can be regarded as happening at the SWNT/IL CNG in air:

$$2\,Li + O_2 \rightleftharpoons Li_2O_2 \tag{1}$$

$$4\,Li + O_2 + 2\,H_2O \rightleftharpoons 4\,LiOH \tag{2}$$

$$2\,LiOH + CO_2 \rightarrow Li_2CO_3 + H_2O \tag{3}$$

$$2\,Li_2O_2 + 2\,CO_2 \rightarrow 2\,Li_2CO_3 + O_2 \tag{4}$$

To determine the contamination by H_2O and CO_2 more accurately, the cyclability of the Li–O_2 and Li–air cells with a limited discharge capacity of 1000 mAh g^{-1} were compared (Figure 3c,d). For the first time, it was observed that the discharge potential of the lithium–air cell began to rise from the fifth cycle, and gradually generated two platforms, unlike the single platform of the Li–O_2 cell during all the 10 cycles. The elevation platform remains stable at about 3.0 V, which is consistent with the discharge potential of the lithium–air battery with an alkaline aqueous electrolyte.[17] These results show explicitly that eliminating the availability of H_2O through the passage of the SWNT/IL CNG is paramount in regard to further practical applications in air. If the H_2O permeation can be prevented, not only can reaction (2) be eliminated, but so can reactions (3) and (4) because they depend strongly on H_2O to take place or to be accelerated.

Thus, it is possible to realize a single reversible cell reaction (1) of $2\,Li + O_2 \rightleftharpoons Li_2O_2$ even in ambient air.

Attempts have been made to suppress the H_2O from the air by introducing another hydrophobic diffusion layer between the CNG and carbon paper current collector. The discharge potential retained the single platforms corresponding only to the reaction of $Li + O_2 \rightarrow Li_2O_2$ during the tested 10 cycles (Figure 4a), thus suggesting that the disturbance of the H_2O has been suppressed by the addition of the hydrophobic diffusion layer. Clearly, to prevent the H_2O contamination completely is beyond the ability of the hydrophobic layer, as illustrated in the inset of Figures 3c,d and 4a. Nevertheless, by alleviating the deleterious effects preliminarily, a significant improvement on the cell performance has been achieved when operated in ambient air (Figure 4b). The lithium–air cell with a hydrophobic diffusion layer and a SWNT/IL CNG exhibited a discharge capacity of 10730 mAh g^{-1} at 2.0 V, and then a completely reversible charge process at about 4.0 V, with a mid-potential deviation of 1.17 V. The key achievement lies in the prominent reversibility with an attractive capacity, polarization, and electrical energy efficiency which have never been reported elsewhere, especially when taking into account the operation conditions of ambient air.

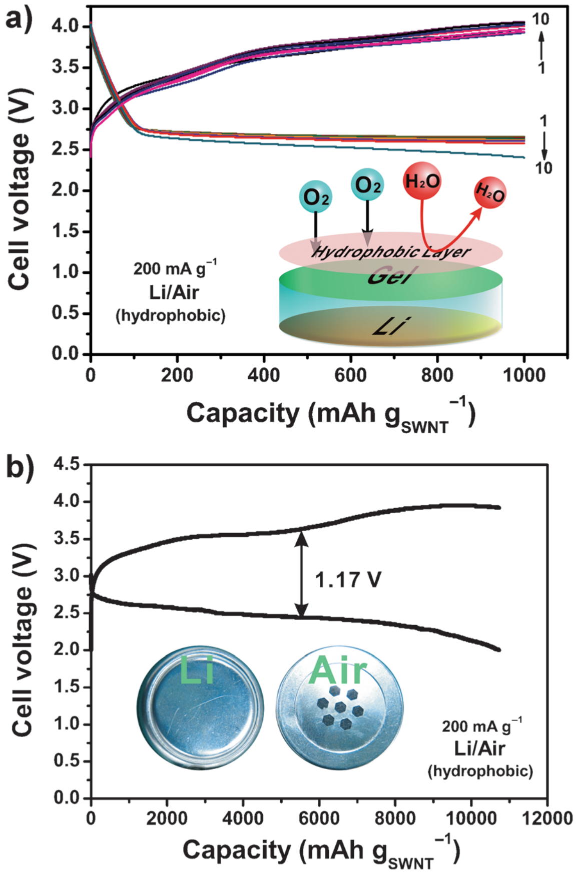

Figure 4. Electrochemical behavior of the Li–air cell with a hydrophobic layer. a) The discharge/charge behavior of the Li–air cells (ambient air) with the SWNT/[C_2C_1im][NTf$_2$] CNG at 200 mA g$_{SWNT}^{-1}$ when the state of discharge was limited to 1000 mAh g^{-1}. b) The discharge/charge curves of the Li–air cells with SWNT/[C_2C_1im][NTf$_2$] CNG at 200 mA g$_{SWNT}^{-1}$ in ambient air. The cut-off voltages were 2.0 V on discharge and ca. 4.0 V on charge. The capacities were all normalized by the weight of the SWNTs. Herein a hydrophobic layer was coated between the CP current collector and SWNT/IL cross-linked gel. The inset in Figure 4a illustrates the effect of the hydrophobic layer on suppressing the contamination by water from the ambient air.

Our research demonstrates that the SWNT/IL CNG allows the superior three-dimensional tricontinuous passage of electrons, ions, and oxygen, which is able to expand the conventional three-phase reactive interface to the whole cross-linked network, and thus integrates the attractive performance of specific energy, specific power, and the feasibility of operating in ambient air for Li–O_2 and Li–air batteries. The untangled SWNTs in the SWNT/IL CNG resulted in the proliferation of available reaction sites, and the anchored IL was sustainable for the expedite passage by suppressing the permeation of the electrolyte. As a consequence, the Li–O_2 cell using the SWNT/IL CNG and the corresponding IL electrolyte exhibited a prominent specific energy density of 2440 Wh kg^{-1}, as well as a specific power density of 1660 W kg^{-1}, based on the weight of the SWNTs and Li_2O_2, the product from the reversible electrochemical reaction of Li and O_2. Furthermore, a reversible discharge and charge capacity of 10730 mAh g^{-1} has also been achieved even in ambient air by alleviating the H_2O contamination, thus revealing a preliminary opportunity to move from Li–O_2 into Li–air cells by utilizing the SWNT/IL CNG. From a broader perspective, the SWNT/IL CNG represents a neoteric gel-state air electrode, which is binder-free, flexible to accommodate discharge products, and has rich possibilities for further manipulation, for example, to tailor the surface of nanotubes by catalysts, to adjust the passage ability of H_2O by additives, and to extend the compatibility to other solvents and salts. There may also be scope for using gel–air electrodes for quasisolid-state Li–air batteries.[18] It is believed that the SWNT/IL CNG reveals a new avenue for the improvement of the three-phase reaction at an air cathode and will result in the study of gel electrodes in the research on lithium–air batteries for long-lived practice application in ambient environments.

Received: June 26, 2012

Keywords: carbon nanotubes · conductivity · gels · ionic liquids · lithium–air batteries

---

[1] P. G. Bruce, S. A. Freunberger, L. J. Hardwick, J.-M. Tarascon, *Nat. Mater.* **2012**, *11*, 19–29.
[2] S. A. Freunberger, Y. Chen, Z. Peng, J. M. Griffin, L. J. Hardwick, F. Bardé, P. Novák, P. G. Bruce, *J. Am. Chem. Soc.* **2011**, *133*, 8040–8047.
[3] a) J. Read, *J. Electrochem. Soc.* **2002**, *149*, A1190–A1195; b) C. Tran, X-Q. Yang, D. Qu, *J. Power Sources* **2010**, *195*, 2057–2063.
[4] a) T. Kuboki, T. Okuyama, T. Ohsaki, N. Takami, *J. Power Sources* **2005**, *146*, 766–769; b) C. J. Allen, S. Mukerjee, E. J. Plichta, M. A. Hendrickson, K. M. Abraham, *J. Phys. Chem. Lett.* **2011**, 2, 2420–2424.
[5] a) K. M. Abraham, Z. Jiang, *J. Electrochem. Soc.* **1996**, *143*, 1–5; b) J. Suntivich, K. J. May, H. A. Gasteiger, J. B. Goodenough, Y. Shao-Horn, *Science* **2011**, *334*, 1383–1385.

[6] a) S. Iijima, T. Ichihashi, *Nature* **1993**, *363*, 603 – 605; b) D. S. Bethune, C. H. Klang, M. S. de Vries, G. Gorman, R. Savoy, J. Vazquez, R. Beyers, *Nature* **1993**, *363*, 605 – 607.
[7] T. Fukushima, A. Kosaka, Y. Yamamoto, T. Aimiya, S. Notazawa, T. Takigawa, T. Inabe, T. Aida, *Small* **2006**, *2*, 554 – 560.
[8] J. Liu, et al., *Science* **1998**, *280*, 1253 – 1256.
[9] T. Fukushima, A. Kosaka, Y. Ishimura, T. Yamamoto, T. Takigawa, N. Ishii, T. Aida, *Science* **2003**, *300*, 2072 – 2074.
[10] Y.-C. Lu, Z. Xu, H. A. Gasteiger, S. Chen, K. Hamad-Schifferli, Y. Shao-Horn, *J. Am. Chem. Soc.* **2010**, *132*, 12170 – 12171.
[11] A. Débart, A. J. Paterson, J. Bao, P. G. Bruce, *Angew. Chem.* **2008**, *120*, 4597 – 4600; *Angew. Chem. Int. Ed.* **2008**, *47*, 4521 – 4524.
[12] Y. Li, J. Wang, X. Li, D. Geng, R. Li, X. Sun, *Chem. Commun.* **2011**, *47*, 9438 – 9440.
[13] Y.-C. Lu, D. G. Kwabi, K. P. C. Yao, J. R. Harding, J. Zhou, L. Zuin, Y. Shao-Horn, *Energy Environ. Sci.* **2011**, *4*, 2999 – 3007.
[14] J. Christensen, P. Albertus, R. S. Sanchez-Carrera, T. Lohmann, B. Kozinsky, R. Liedtke, J. Ahmed, A. Kojic, *J. Electrochem. Soc.* **2012**, *159*, R1 – R30.
[15] G. Girishkumar, B. McCloskey, A. C. Luntz, S. Swanson, W. Wilcke, *J. Phys. Chem. Lett.* **2010**, *1*, 2193 – 2203.
[16] J. Xiao, et al., *Nano Lett.* **2011**, *11*, 5071 – 5078.
[17] E. Yoo, H. Zhou, *ACS Nano* **2011**, *5*, 3020 – 3026.
[18] Y. Wang, H. Zhou, *Energy Environ. Sci.* **2011**, *4*, 1704 – 1707.